Off-axis wave front measurements for optical correction in eccentric viewing

Linda Lundström
Peter Unsbo
Royal Institute of Technology
Biomedical and X-Ray Physics
Department of Physics
Stockholm, Sweden

Jörgen Gustafsson
Lund University
Certec, Rehabilitation Engineering Research
Department of Design Sciences
Lund, Sweden

Abstract. In a previous study we have shown that correction of peripheral refractive errors can improve the remaining vision of subjects with large central visual field loss. Measuring peripheral refractive errors with traditional methods is often difficult due to low visual acuity and large aberrations. Therefore a Hartmann–Shack sensor has been designed to measure peripheral wave front aberrations in subjects using eccentric viewing. The sensor incorporates an eye tracker and analyzing software designed to handle large wave front aberrations and elliptic pupils. To ensure that the measurement axis is aligned with the direction of the subject's preferred retinal location, a special fixation target has been developed. It consists of concentric rings surrounding the aperture of the sensor together with a central fixation mark along the measurement axis. Some initial measurements on subjects using eccentric viewing have been performed successfully. As a first step in improving the peripheral optics of the eye, the wave front has been used to calculate the eccentric refraction. This refraction has been compared to the refraction found with the PowerRefractor instrument. Measuring the off-axis wave front is a fast way to assess the optical errors in the subject's eccentric viewing angle and to better understand the problems of eccentric correction. [DOI: 10.1117/1.1920587]

Keywords: vision; peripheral wave front aberrations; Hartmann–Shack sensor; PowerRefractor; central visual field loss; eccentric viewing; preferred retinal location; eccentric refraction; Strehl ratio.

Paper 04080RR received May 19, 2004; revised manuscript received Nov. 30, 2004; accepted for publication Dec. 2, 2004; published online Jun. 1, 2005. This paper is a revision of a paper presented at the SPIE conference on Ophthalmic Technologies XIV, Jan. 2004, San Jose, CA. The paper presented there appears (unrefereed) in SPIE Proceedings Vol. 5314.

1 Introduction

Central visual field loss (CFL) is an increasing problem in the aging population and magnifying devices are currently the only help for affected persons to use their remaining visual function. However, we have recently shown that the remaining vision for these people can be improved by correcting peripheral defocus and astigmatism.[1,2] The aim of the current work is to more thoroughly evaluate eccentric corrections. We have therefore developed a Hartmann–Shack (HS) technique to measure the peripheral wave front aberrations of individuals with CFL.

In an eye with dense or absolute CFL, the fovea is not working and the person has to rely on peripheral vision. Some people with CFL can utilize their remaining vision better by actively using eccentric viewing, i.e., using a certain part of the peripheral retina, a so called preferred retinal location. Peripheral vision can never fully replace direct or central vision, but with eccentric viewing people with CFL can, to a limited extent, perform visual tasks such as reading or watching television. CFL is the result of a variety of pathologies, like atrophy in the nervus opticus, but the most common cause of CFL is age-related macula degeneration and this problem is increasing as the population gets older. It is estimated today that about eight million people worldwide are severely visually impaired due to macula degeneration.[3] In the USA age-related macula degeneration was found in 5% of the population age 65 and older.

Vision in eccentric viewing angles is limited both by the resolution capacity of the peripheral retina and by the large aberrations in the peripheral optics of the eye. It has commonly been assumed that the main limitation is poor retinal capacity and the only help prescribed to CFL patients has been magnifying devices. However, in a previous study we have shown that the remaining vision of subjects with CFL, using a well-defined preferred retinal location, can be improved by correcting the peripheral optical errors.[1,4]

Measuring the peripheral optics and refractive errors with traditional methods in subjects with CFL is often difficult due to the large aberrations, reduced retinal function and poor fixation. In the earlier-mentioned study, off-axis refractive er-

Address all correspondence to Linda Lundström, KTH ALBANOVA, Biomedical and X-Ray Physics, Roslagstullsbacken 21, SE-106 91 Stockholm, Sweden. Tel: +46 (0)8 55 37 81 24; Fax: +46 (0)8 55 37 87 98; E-mail: linda@biox.kth.se

1083-3668/2005/$22.00 © 2005 SPIE

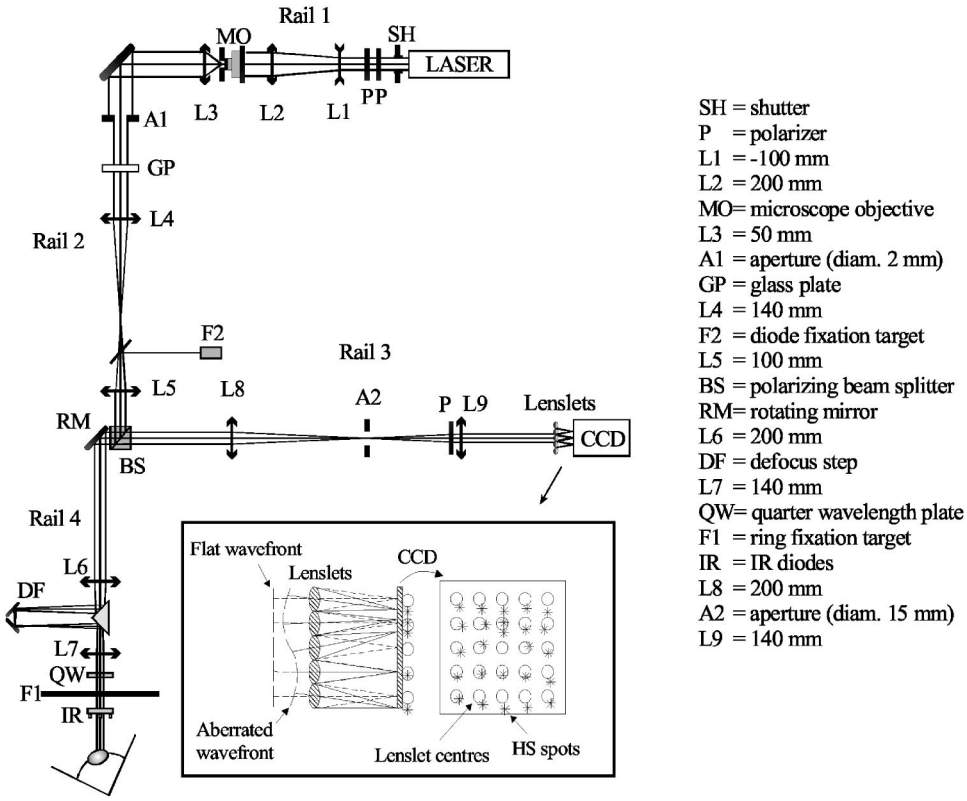

Fig. 1 The HS setup with descriptions. The inset shows the principle of the HS sensor. The lenslet array consists of lenslets 325×325 μm in size, with a focal length of 18 mm. Each lenslet covers about 50×50 pixels on the charge coupled device detector in the focal plane of the lenslets.

rors were measured by photorefraction with the PowerRefractor instrument[5,6] and a special fixation target was developed to help the subject hold a stable fixation. Other methods used to investigated peripheral refraction and oblique astigmatism are: the Zeiss parallax optometer,[7–9] the Hartinger optometer,[10] retinoscopy,[11] and the double-pass method.[12–17] However, all of these methods only give the spherical and cylindrical correction (even though the double-pass method can give an indirect measurement of the higher order aberrations via the point-spread function). In large eccentric viewing angles of 20°–30° off-axis, the oblique astigmatism and higher order aberrations are considerably larger.[18,19] There is thus a need for methods that give more detailed information about the peripheral optics of the eye.

A way to assess more detailed information about the optical system of the eye is to measure the total wave front aberrations with a HS sensor. Atchison et al.[19] have previously reported measurements of peripheral wave front aberrations in normal subjects with a HS sensor. In the present paper we describe a HS sensor adapted to measure the off-axis wave front of subjects with large CFL. The measurement method incorporates special fixation targets, an eye tracker, and analyzing software. The special software has been designed to handle the elliptic pupil and the large wave front aberrations, and to calculate how the retinal point-spread function can be improved with different corrections. This paper describes the setup and software and gives examples of measurements on subjects with CFL.

2 Method

The HS sensor has been designed to measure the eccentric wave front aberrations of the eye. The principle of the optical setup resembles a traditional HS sensor for foveal measurements[20] with the pupil of the eye imaged onto a lenslet array (Sec. 2.1). The setup incorporates fixation targets to enable subjects with CFL to use eccentric viewing and align the measurement axis with the direction of the preferred retinal location. An eye tracker is also built into the system to follow the angle of gaze and the position of the eye. The raw data from the HS sensor is handled by software, specially developed for this purpose (Secs. 2.2. and 2.3). As a first step the eccentric refraction is calculated from the wave front data and compared to the refraction found with the PowerRefractor instrument.[1,2,4–6] All measurements on subjects followed the Declaration of Helsinki and were approved by the local Research Ethics Committee. The subjects gave informed consent prior to participation.

2.1 *The Hartmann–Shack Setup*

Figure 1 and the photo in Fig. 2 show the optics of the HS setup, which also includes relay lenses imaging the pupil of the eye in the same conjugate plane as the lenslet array. The light source is a helium–neon laser (5 mW at 633 nm), the exposure time is typically around 200 ms and the collimated laser beam entering the eye has an intensity of 30 μW, which is about one tenth of the recommended safety limits.[21] The

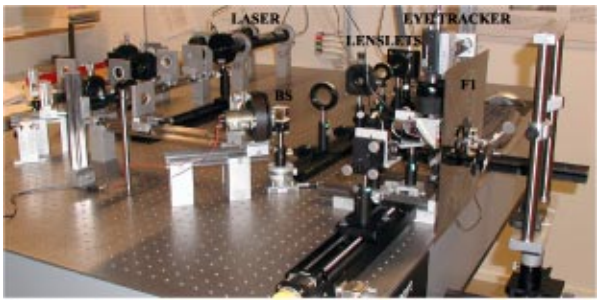

Fig. 2 Photo of the HS setup. Eye tracker camera, ring fixation target, IR diodes, and headrest can also be seen.

setup incorporates a fast rotating mirror to avoid speckles and an adjustable defocus step to compensate for large amounts of defocus. To optimize the amount of reflected light from the retina to the detector and minimize the reflexes from the lenses a quarter-wave plate, a polarizing beamsplitter, and a polarizer are used.

When measuring the peripheral wave front aberrations of an eye with CFL, it is essential that the measurement is performed in the direction that the subject normally uses for eccentric viewing. That is, the measurement axis of the HS sensor has to be aligned with the direction of the subject's preferred retinal location. It is also important that the eye does not move, so that the measurement can be repeated. Two special fixation targets have therefore been developed to enable the subject to look in the correct direction and keep a stable fixation. The first fixation target ($F1$ in Fig. 1) consists of multicolored shining rings around the axis of the HS sensor (see Fig. 3). The subject will only see the parts of the ring pattern outside his/her scotoma (the dysfunctional region of the retina) and can thus be helped by the rings to place the scotoma in a certain direction and hold it steady. The same principle was used during the measurements with the PowerRefractor both in this study and in a previous study.[1] Due to space limitations the target is placed very close to the eye, about 100 mm, which makes it unsuitable for normal, healthy eyes since it might stimulate accommodation. However, this is not the case for subjects with central visual field loss since they fixate eccentrically to the second fixation target ($F2$ in Fig. 1) and only use the rings as orientation help. The second target is a green diode aligned with the measurement axis of the HS sensor via a beamsplitter. The subject should try to direct his/her eye so that the green light is seen as clearly as possible, i.e., placed in the preferred retinal location. Since the peripheral retina has limited resolution capacity, this central fixation mark is large and is thus not suitable as a foveal fixation target.

Fig. 3 The fixation target with ring patterns seen through the headrest.

Like most HS sensors this setup has a pupil camera, which helps the examiner to move the subject's eye to the correct position for the HS sensor. The camera has an additional purpose as an eye tracker that measures the angle of gaze of the eye. The novel eye tracker software (Tobii Technology Inc.®) is specially developed to track an eccentric pupil in real time and to save the data of the images, the pupil shape, and the angle of gaze. The pupil camera uses the illumination from infrared (IR) diodes and finds the direction of the eye either from the elliptic shape of the pupil or from the specular reflexes from the diodes in the cornea. The angle of gaze data is needed to make sure that the wave front is measured in the same angle as the subject normally uses and that the fixation direction remains constant between the measurements.

2.2 *Wave Front Reconstruction*

After a measurement the HS image has to be computer processed to find the displacements of the spots and the shape of the wave front. For this purpose we have developed a software package in Matlab® that solves a number of problems associated with measuring the wave front aberrations in eccentric angles. The software differs from that of conventional HS sensors especially in how the unwrapping is performed and how the pupil shape is taken into consideration.

First of all, the HS image is processed to find the location of the centroids of the spots.[22] The resulting spot pattern must then be unwrapped, i.e., for each spot the corresponding lenslet has to be identified. This puts a limit on the measurable shape of a wave front; if a spot has moved outside the region of its lenslet and closer to another lenslet, it will be more difficult to assign the spot to the correct lenslet—the so called unwrapping problem. To be able to measure large aberrations, we have developed a software-based unwrapping algorithm.[23] The algorithm uses a two dimensional B-spline polynomial to predict the deviation between a HS spot and a lenslet. It first connects the central 3×3 HS spots with the closest lenslets, performs a least squares fit to the deviations, and then extrapolates to the closest not-yet-connected lenslets. The algorithm continues outwards in circles in an iterative manner and is able to work around difficult parts in the HS spot pattern and handle missing HS spots [an example of this is seen in Fig. 4(c)].

The deviations of the HS spots divided by the focal length of the lenslets give the local tilts of the wave front. This algorithm uses modal reconstruction with a least squares fit of Zernike coefficients to reconstruct the wave front.[24] The Zernike polynomials, Z_n^m (where n is the radial order and m is

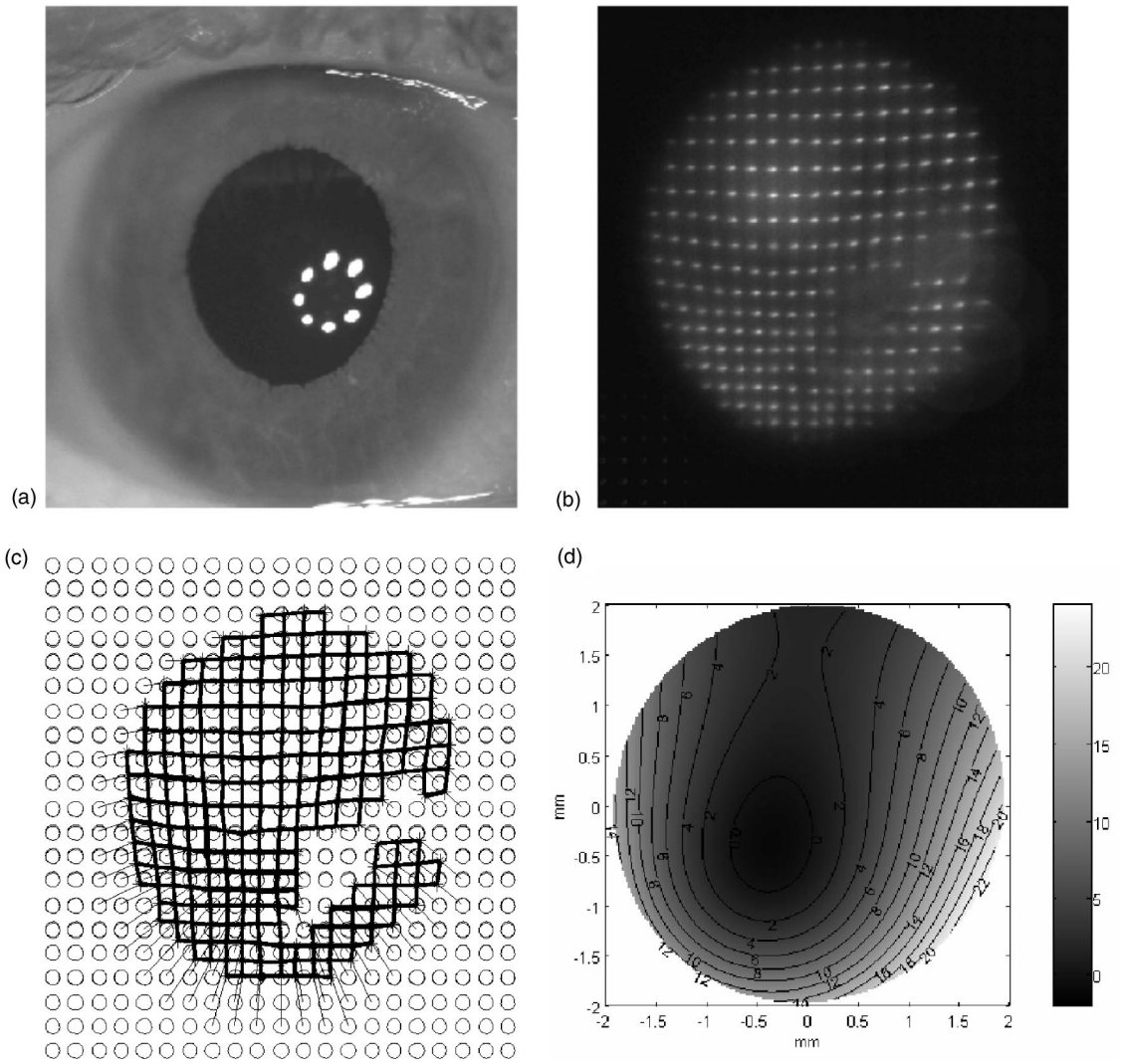

Fig. 4 Example of a wave front measurement on subject *D* showing (a) the image from the eye tracker and (b) the original HS image. In (c) the spot pattern is unwrapped and each HS spot (star) is connected to its corresponding lenslet (circle). In (d) the wave front is reconstructed from the average of seven separate measurements (the height of the wave front is in micrometers).

the azimuthal frequency)[25,26] constitute a complete, orthogonal set of polynomials defined over a unit circle. Thus, any physical wave front Φ can be expanded into Zernike polynomials

$$\Phi(x,y)=\sum_{n,m} c_n^m Z_n^m(x,y),$$

where c_n^m are the Zernike coefficients (in micrometers) and (x,y) are normalized coordinates in the pupil plane. When eccentric wave front aberrations are reconstructed, a complication arises since the pupil and the wave front will be elliptic while the Zernike polynomials are defined over a circle. We have solved this by reconstructing the wave front over a circle with a radius equal to the major axis of the elliptic pupil. There will thus be an extrapolated part of the wave front outside the pupil that has no physical relevance. When the aberrations are evaluated, this part is removed. To verify that the calculated Zernike coefficients describe the measured HS spot pattern within the pupil, the algorithm calculates backwards from the wave front described by the coefficients to the spot pattern it would generate. This spot pattern is then compared to the originally measured spot pattern.

Multiple wave front measurements are made to minimize the influence of fluctuations in the higher order aberrations, due to the tear film, minor changes in fixation direction, etc. The Zernike coefficients are calculated for each measurement and are then averaged to describe the off-axis wave front of the eye. It is thus very important to measure in the same angle each time and the eye tracker gives a good indication of whether two measurements can be averaged or not.

2.3 *Wave Front Evaluation*

The shape of the wave front describes the optics of the eye and can be used to evaluate different optical corrections. The aim is to give the subject as good vision as possible with available corrections, i.e., refractive correction with spectacles or contact lenses. An important problem is to know what ''as good vision as possible'' means and thus by which metric to

optimize. The metrics available are usually divided into two groups: pupil plane metrics, based directly on the wave front aberrations, and image plane metrics, where the wave front aberrations are computed further to calculate the retinal image. According to Guirao et al.[27] the image plane metrics corresponds well with subjective impressions for normal foveal vision, while the pupil plane metrics give a poor prediction, especially when the aberrations are large.

One pupil plane method, which is currently often used to find the optimum correction in foveal vision, minimizes the root-mean-square (rms) of the wave front error. The refractive correction can in this case simply be calculated from the second order Zernike coefficients c_2^{-2}, c_2^0, c_2^2:

$$M = -\frac{4\sqrt{3}}{r_{pupil}^2} c_2^0, \quad J_{0^\circ} = -\frac{2\sqrt{6}}{r_{\text{pupil}}^2} c_2^2, \quad J_{45^\circ} = -\frac{2\sqrt{6}}{r_{\text{pupil}}^2} c_2^{-2},$$

where the coefficients are in micrometers and the radius of the pupil, r_{pupil}, is in millimeters to yield the refraction in diopters. In the equations above the refractive correction is expressed as an astigmatic decomposition with spherical equivalent, M, one Jackson cross-cylinder component with axis 0°, J_{0°, and one Jackson cross-cylinder component with axis 45°, J_{45°.[28] These can be translated into traditional sphere, cylinder, and axis in the following manner:

$$\text{cylinder} = -2\sqrt{J_{0^\circ}^2 + J_{45^\circ}^2},$$

$$\text{axis} = \arctan\left(\frac{\text{cylinder} + 2J_{0^\circ}}{-2J_{45^\circ}}\right) \quad \text{if axis} < 0 \ \text{ add } 180^\circ,$$

$$\text{sphere} = M - \frac{\text{cylinder}}{2}.$$

Our algorithm uses an image plane method with optimization of the point-spread function, which is a description of the retinal image of a point-like object. The point-spread function is found by Fourier transformation of the generalized pupil function $\boldsymbol{P}(x,y)$[29]:

$$\text{PSF} = \frac{|\mathfrak{F}\{\boldsymbol{P}(x,y)\}|^2}{\text{pupil area}},$$

$$\boldsymbol{P}(x,y) = \Pi(x,y) \cdot e^{-i2\pi/\lambda \Phi(x,y)},$$

where x and y are the coordinates in the pupil. The generalized pupil function includes the height of the measured wave front, $\Phi(x,y)$, and the shape of the pupil, $\Pi(x,y)$, which equals one inside the pupil and zero outside. The elliptic shape of the pupil is thus taken into consideration with this calculation, since only the wave front inside the pupil is used for computing the point-spread function. The pupil shape can be taken from either the eye tracker or the HS image. The Strehl ratio, i.e., the peak value of the point-spread function normalized by the diffraction limited point-spread function, is then optimized by trial and error. A wide range of combinations of spherical and cylindrical corrections are stepped through and the Strehl ratio for each combination is computed. The sphere and cylinder values are chosen $\pm 10\,D$ in $0.1\,D$ steps around the minimum rms-correction of the circular wave front. The combination that gives the largest Strehl ratio is regarded as the optimum one. This method is not limited to spherical and cylindrical values; it can also be used to optimize various aberration corrections.

3 Results

The HS sensor and the software have been tested successfully in eccentric viewing angles on six subjects with CFL. The subjects have found the fixation targets to be a useful help to align their preferred retinal location with the measurement axis of the sensor and to keep their fixation stable. It was thus possible to make multiple measurements in the preferred retinal location of each subject. The quality of the HS images is good, without disturbing reflexes and stray light, and the wave fronts have been successfully unwrapped and reconstructed. The measured aberrations and the pupil sizes have been used to find optimal spherical and cylindrical corrections by optimizing the Strehl ratio.

In Table 1 the eccentric refractions found with the HS sensor and the refractions found with the PowerRefractor are listed for all subjects together with the direction of their preferred retinal location. A comparison of the refractions shows that the HS sensor generally has measured a more oblique axis of the astigmatism (larger J_{45°) and that the PowerRefractor found a larger total cylinder for all subjects except subject *D*. The equivalent sphere is approximately unchanged for subject *A*, *B*, *C*, and *F*. As an example the HS measurements of subject *D* is presented more in detail. Subject *D* is a man born 1962 with a large CFL of radius of about 20° (stable the last 5 years). His right eye has a well trained preferred retinal location approximately 20° in the horizontal nasal visual field. Seven measurements in his preferred retinal location has been preformed in a dark room with a natural pupil (no cycloplegia was used). Only the ring pattern fixation target was in use during the measurements, since the central diode fixation target was not yet implemented. He commented that it was much easier to keep the eye stable with the fixation target than without. Table 2 shows that his fixation was stable during all measurements, which were all taken within half an hour. The results from the HS measurements on subject *D* are presented in Fig. 4. The first three images show the eye tracker image, the original HS image and the unwrapped HS spot pattern for the first measurement. The missing spots in the pupil are due to opacities in the eyes optical media. Figure 4(d) is the wave front reconstructed from the average Zernike coefficients of all seven measurements. The optimum spherical and cylindrical refraction is $M = -4.25\,D$, $J_{0^\circ} = -0.80\,D$, and $J_{45^\circ} = 0.96\,D$ with the Strehl method calculated for a pupil size of 4 mm.

4 Summary and Discussion

We have recently shown that the remaining vision of subjects with CFL can be improved by correcting the eccentric refractive errors in the fixation direction of the preferred retinal location.[1,2,4] The peripheral optics of the eye often suffers from large aberrations, and this together with the low visual acuity makes it more difficult to assess the required correction with traditional subjective methods for foveal vision. The technique we have developed measures the wave front aberrations in the subject's preferred retinal location with an ob-

Table 1 The eccentric corrections in the preferred retinal location for the six subjects with central visual field loss and eccentric viewing. For each subject the preferred retinal location of the best eye is given as an angle in the visual field. The eccentric refractions are measured with the PowerRefractor instrument and with the developed Hartmann–Shack technique with the same type of ring fixation target. For subject *A* the PowerRefractor could not measure in the preferred retinal location, instead a slightly smaller angle has been used. Subject *A* has earlier been described in Ref. 4, and in Ref. 1 subject *A* is subject No. 1 and subject *B* is No. 2.

		Ecc corr PowerRefractor			Ecc HS corr		
Subject	Preferred retinal location	M	$J_{0°}$	$J_{45°}$	M	$J_{0°}$	$J_{45°}$
A	OD 35° nasally	2.00	−2.00	0.00	2.00	−0.94	−0.34
B	OS 20° temporally	−3.50	−1.50	0.00	−4.13	−0.82	0.30
C	OS 10° down	−0.75	1.64	−0.60	−0.75	1.23	0.22
D	OS 20° nasally	−4.25	−0.80	0.96	−2.75	−0.78	4.43
E	OD 15° nasally	−1.75	−1.00	0.00	−4.00	−0.70	0.26
F	OD 20° nasally	0.00	−1.50	0.00	−0.50	−1.00	0.00

jective HS sensor designed for peripheral measurements. The software package includes a special unwrapping algorithm and the wave front from the elliptic pupil is reconstructed with Zernike polynomials defined over a circle, which encloses the pupil. In the subsequent trial and error procedure the wave front is cut so that only the central elliptic wave front is used to find the refractive correction, which optimizes the Strehl ratio. The main advantage with this method is that it takes all aberrations within the elliptical pupil into consideration. The higher order aberrations contain components resembling defocus and astigmatism and will thus affect the refraction, especially when the aberrations are large. Another advantage with the Strehl method and the trial and error process is that it will not be mislead by, what optics designers call, local minima. A local minimum for a certain correction means that the retinal image quality is better here compared to what it is for other, slightly different corrections. But if the correction is changed more radically, another minimum can be found with even better image quality. In the peripheral optics of the eye, the higher order aberrations increase the risk of being trapped in a local minimum. The trial and error technique avoids this by objectively comparing a wide range of corrections. Maximizing the Strehl ratio is not the only metric that can be used. Other retinal image plane metrics, as for example the intensity variance of the point-spread function or the volume of the modulation transfer function in certain regions of spatial frequencies, may also be useful.[27] Mouroulis et al.[30] suggest that the maximum Strehl ratio might be misleading if the aberrations are very large and the Strehl ratio is very low.

The measurement technique differs from that of Atchison et al.[19] in the design of the fixation targets, in the unwrapping algorithm and in how the elliptical pupil is handled. Atchison stretched the coordinates of the pupil to a circular shape before the wave front reconstruction; we leave parts of the circular Zernike pupil without sampling points and only use the sampled parts when evaluating the Strehl value. This means that the Zernike coefficients cannot be used directly to find either the rms of the wave front error or the refraction that minimizes the rms. However, the backwards calculation, from the coefficients to the HS spot pattern, confirms that the Zernike coefficients give a good description of the central elliptic wave front. A simulation has also been performed to verify that the extrapolated parts of the Zernike wave front do not affect the reconstruction of the central elliptic wave front. In the simulation the spot pattern from a circular pupil was reconstructed both with the correct pupil size and with a pupil diameter 50% larger. In the second case the wave front was therefore extrapolated, since there were only spots in the central part of the large pupil. The central part of this extrapolated wave front was then cut out by recalculating the Zernike coefficients to the correct size.[31] The resulting coefficients were equal to the coefficients that were calculated from the spot pattern with the correct pupil size. These simulations

Table 2 Subject *D*'s angle of fixation for each measurement in spherical coordinates. φ is the direction angle (0°=left, 90°=up, etc.) and θ is the eccentricity angle (0°=the central visual axis of the eye is aligned with the HS axis). The eye tracker was running in an uncalibrated mode, there may thus be a shift in the actual angles.

Measurement	1	2	3	4	5	6	7
φ	152°	160°	164°	156°	153°	164°	153°
θ	16°	15°	16°	15°	17°	19°	17°

were performed on real measurements with large aberrations and we therefore conclude that the extrapolation process does not influence the reconstructed wave front.

As a first step the CFL subjects have been prescribed spherical and cylindrical corrections based on peripheral wave front measurements. The eccentric refractive correction in the subjects preferred retinal location has also been measured with the PowerRefractor as is shown in Table 1. The correction found with the HS sensor is used instead of that from the PowerRefractor, because the PowerRefractor has proven to be more inaccurate in oblique angles and cannot be used at all in larger angles.[5,6]

For subject *A* the PowerRefractor could not measure in the preferred retinal location since it was too far off-axis, instead a slightly smaller angle was used. The differences found in the comparison between the PowerRefractor and the HS sensor might be explained by the fact that the HS sensor measures all aberrations, while it is not well documented how the PowerRefractor handles large higher order aberrations. This might also explain why subject *D*, who has large amounts of coma-like aberrations, showed a very large difference in astigmatism between the two methods. Another advantage with the HS technique is that it can also be used to optimize aberration corrections. The largest higher order aberration in the periphery is coma[17,19] and it would therefore be interesting to investigate if a coma correction could improve the visual function of subjects with CFL.

Acknowledgments

The financial support for this research, provided by the Göran Gustafsson Foundation, the Carl Trygger Foundation, and the Carl-Johan and Berit Wettergren Foundation, is greatly appreciated.

References

1. J. Gustafsson and P. Unsbo, ''Eccentric correction for off-axis vision in central visual field loss,'' *Optom. Vision Sci.* **7**, 535–541 (2003).
2. J. Gustafsson, ''Optics for low vision enabling,'' PhD thesis, Lund University, Sweden (2004).
3. R. Leonard, *Statistics on Vision Impairment: A Resource Manual*, Arlene R. Gordon Research Institute of Lighthouse International (2002).
4. J. Gustafsson, ''The first successful eccentric correction,'' *Visual Impairment Research* **3**, 147–155 (2002).
5. M. Choi, S. Weiss, F. Schaeffel, A. Seidemann, H. C. Howland, B. Wilhelm, and H. Wilhelm, ''Laboratory, clinical, and kindergarten test of a new eccentric infrared photorefractor (PowerRefractor),'' *Optom. Vision Sci.* **77**, 537–548 (2000).
6. A. Seidemann, F. Schaeffel, A. Guirao, N. Lopez-Gil, and P. Artal, ''Peripheral refractive errors in myopic, emmetropic, and hyperopic young subjects,'' *J. Opt. Soc. Am. A* **19**, 2363–2373 (2002).
7. C. E. Ferree, G. Rand, and C. Hardy, ''Refraction for the peripheral field of vision,'' *Arch. Ophthalmol. (Chicago)* **5**, 717–731 (1931).
8. C. E. Ferree, G. Rand, and C. Hardy, ''Refractive asymmetry in the temporal and nasal halves of the visual field,'' *Am. J. Ophthalmol.* **15**, 513–522 (1932).
9. C. E. Ferree and G. Rand, ''Interpretation of refractive conditions in the perpheral field of vision,'' *Arch. Ophthalmol. (Chicago)* **9**, 925–938 (1933).
10. M. Millodot, ''Effect of ametropia on peripheral refraction,'' *Am. J. Optom. Physiol. Opt.* **58**, 691–695 (1981).
11. F. Rempt, J. Hoogerheide, and W. P. H. Hoogenboom, ''Peripheral retinoscopy and the skiagram,'' *Ophthalmologica* **162**, 1–10 (1971).
12. J. A. M. Jennings and W. N. Charman, ''Off-axis image quality in the human-eye,'' *Vision Res.* **21**, 445–455 (1981).
13. J. A. M. Jennings and W. N. Charman, ''Optical image quality in the peripheral retina,'' *Am. J. Optom. Physiol. Opt.* **55**, 582–590 (1978).
14. R. Navarro, P. Artal, and D. R. Williams, ''Modulation transfer of the human eye as a function of retinal eccentricity,'' *J. Opt. Soc. Am. A* **10**, 201–212 (1993).
15. P. Artal, A. M. Derrington, and E. Colombo, ''Refraction, aliasing, and the absence of motion reversals in peripheral vision,'' *Vision Res.* **35**, 939–947 (1995).
16. J. A. M. Jennings and W. N. Charman, ''Analytical approximation of the off-axis modulation transfer function of the eye,'' *Vision Res.* **37**, 697–704 (1997).
17. A. Guirao and P. Artal, ''Off-axis monochromatic aberrations estimated from double pass measurements in the human eye,'' *Vision Res.* **39**, 207–217 (1999).
18. J. Gustafsson, E. Terenius, J. Buchheister, and P. Unsbo, ''Peripheral astigmatism in emmetropic eyes,'' *Ophthalmic Physiol. Opt.* **21**, 393–400 (2001).
19. D. Atchison and D. Scott, ''Monochromatic aberrations of human eyes in the horizontal visual field,'' *J. Opt. Soc. Am. A* **19**, 2180–2184 (2002).
20. J. Liang, B. Grimm, S. Goelz, and J. F. Bille, ''Objective measurement of wave aberrations of the human eye with the use of a Hartmann-Shack wave-front sensor,'' *J. Opt. Soc. Am. A* **11**, 1949–1957 (1994).
21. The Swedish Radiation Protection Institute's Regulations on Lasers, SSI FS 1993:1 (1993).
22. L. Lundström, P. Unsbo, and J. Gustafsson, ''Measuring peripheral wavefront aberrations in subjects with large central visual field loss,'' *Proc. SPIE* **5314**, 209–219 (2004).
23. L. Lundström and P. Unsbo, ''Unwrapping Hartmann-Shack images from highly aberrated eyes using an iterative B-spline based extrapolation method,'' *Optom. Vision Sci.* **81**, 383–388 (2004).
24. R. Cubalchini, ''Modal wave-front estimation from phase derivative measurements,'' *J. Opt. Soc. Am. A* **69**, 972–977 (1979).
25. L. N. Thibos, R. A. Applegate, J. T. Schwiegerling, R. Webb, and VSIA Standards Taskforce Members, ''Standards for reporting the optical aberrations of eyes,'' in ''Trends in optics and photonics,'' V. Lakshminarayanan, *Vision Science and Its Applications* **35**, pp. 232–244, OSA Technical Digest Series, Washington, DC (2000).
26. D. Malacara, *Optical Shop Testing*, Wiley, New York (1992).
27. A. Guirao and D. R. Williams, ''A method to predict refractive errors from wave aberration data,'' *Optom. Vision Sci.* **80**, 36–42 (2003).
28. L. N. Thibos, W. Wheeler, and D. Horner, ''A vector method for the analysis of astigmatic refractive errors,'' *Vision Science and Its Applications* **2**, 14–17 (1994).
29. J. W. Goodman, ''Frequency analysis of optical imaging systems,'' in *Introduction to Fourier Optics*, Chap. 6, pp. 126–171, McGraw-Hill, New York (1996).
30. P. Mouroulis and H. Zhang, ''Visual instrument image quality metrics and the effects of coma and astigmatism,'' *J. Opt. Soc. Am. A* **9**, 34–42 (1992).
31. J. Schwiegerling, ''Scaling Zernike expansion coefficients to different pupil sizes,'' *J. Opt. Soc. Am. A* **19**, 1937–1945 (2002).